Catena 234 (2024) 107596

Contents lists available at ScienceDirect

Catena

journal homepage: www.elsevier.com/locate/catena

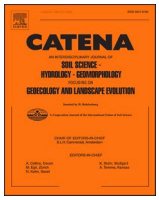

Towards multi-model soil erosion modelling: An evaluation of the erosion potential method (EPM) for global soil erosion assessments

Nejc Bezak [a,*], Pasquale Borrelli [b,c], Matjaž Mikoš [a], Mateja Jemec Auflič [d], Panos Panagos [e]

[a] University of Ljubljana, Faculty of Civil and Geodetic Engineering, Ljubljana, Slovenia
[b] Department of Environmental Sciences, Environmental Geosciences, University of Basel, Basel, Switzerland
[c] Department of Science, Roma Tre University, Rome, Italy
[d] Geological Survey of Slovenia, Ljubljana, Slovenia
[e] European Commission, Joint Research Centre (JRC), Ispra, Italy

ARTICLE INFO

Keywords:
Global assessment
Erosion potential model (EPM)
Soil erosion
Modified erosion potential model (mEPM)
Sediment yield
Model evaluation

ABSTRACT

Soil erosion is expected to increase in the future due to climate change. Soil erosion models are useful tools that can be used by decision makers and other stakeholders to deal with soil erosion problems or the implementation of soil protection measures. Most of the modelling applications are using Universal Soil Loss Equation (USLE)-type models. In this study, we evaluate the applicability of the Erosion Potential Model (EPM) and its modified version (mEPM) for the estimation of the gross and net erosion rates at a global scale. The sensitivity analysis shows that the model results have the highest variability due to the soil protection (land cover) coefficient followed by the soil erodibility parameter. The models' evaluations indicate that that the EPM cannot be applied to cold regions while the mEPM overcomes this issue. The erosion rates based on the EPM were 1.5–2.5 times larger than the ones obtained from the mEPM. Increasing the number of catchment properties as inputs to the model may help in improving the performance of the tested EPM and mEPM. Moreover, a comparison of net soil losses by mEPM with long-term suspended sediment yield data for 116 catchments located around the globe indicates a median bias of less than 10%, although the bias for around 1/3 of catchments was above 100%. Furthermore, a direct comparison with other soil erosion models such as USLE-type models is not possible since the EPM and mEPM do take into consideration other processes such as soil slumps and gully erosion and not just sheet and rill erosion. Therefore, as expected, the gross erosion rates by the EPM and mEPM are higher compared to the USLE-type models. Hence, the mEPM, despite its limitations, could be regarded as an interesting approach for the describing erosion processes around the globe and should be further tested using small- and medium-sized catchments from various climate zones.

1. Introduction

Soil erosion is one of the major environmental threats (Amundson et al., 2015) that is forecasted to diffusely increase under the impact of climate change (Borrelli et al., 2022; Panagos et al., 2022). As soil erosion is a major threat for food security and sustainable provision of ecosystem services, global assessments may provide scientific evidence about the magnitude of the problem. Soil erosion assessments are also included in the recent Intergovernmental Panel for Climate Change (IPCC) reports on the impacts of climate change in land degradation (e.g., Chapter 4 of the Special Report on Climate Change and Land). Despite the recent United Nation efforts (Global Soil Erosion map project, (FAO, 2019)), no coordinated supranational soil erosion monitoring programme exists yet. In many parts of the world soil erosion monitoring is not performed regularly, therefore global modelling applications can be useful to understand the extent of soil erosion and its impact on the environment. Moreover, global modelling applications are also needed to identify areas that are most vulnerable to soil erosion and design conservation and mitigation measures against soil erosion (Borrelli et al., 2021). The motivation in this research comes from the need to provide scientific evidence about the global soil erosion issue and contribute to better accessing the extent of soil erosion in most vulnerable zones.

Therefore, current knowledge on soil erosion dynamics around the globe mostly relies on models, which despite limitations (Alewell et al., 2019), proved to be useful tools being used by different stakeholders for

* Corresponding author.
E-mail address: nejc.bezak@fgg.uni-lj.si (N. Bezak).

https://doi.org/10.1016/j.catena.2023.107596
Received 13 July 2023; Received in revised form 9 October 2023; Accepted 11 October 2023

land management needs to reach soil conservation objectives (USDA, 2019). Additionally, large-scale soil erosion models can be used to highlight large-scale erosion hotspots across the globe, an information useful to support local scale monitoring efforts and, in turn, to evaluate and refine the performance of soil erosion protection measures (Montgomery, 2007). However, it is relevant to remark that most of soil erosion models currently in use (Borrelli et al., 2021) were originally developed for small-scale assessments or using data from small experimental plots (Renard et al., 1997). Hence, these models need to be fully evaluated and tested (Alewell et al., 2019; Bezak et al., 2021; Kirkby et al., 1996).

It is also worth stressing that most of the the global soil erosion modelling applications were carried out using Universal Soil Loss Equation (USLE) or its revised versions (e.g., RUSLE) (Batjes, 1996; Borrelli et al., 2017; Yang et al., 2003) (Borrelli et al., 2021). Only a few global or continental studies applied models other than those belonging to the USLE-type, such as Water Erosion Prediction Project (WEPP) (Laflen et al., 1991), WaTEM/SEDEM (Van Oost et al., 2000), Rangeland Hydrology and Erosion Model (RHEM) (Nearing et al., 2011) or Pan-European Soil Erosion Risk Assessment (PESERA) (Kirkby et al., 2008). Therefore, other soil erosion model types need to be thoroughly tested for large-scale soil erosion assessments. On top, other soil erosion processes (e.g., gully erosion, wind erosion) must be addressed also at global scale. The concept of multiple soil erosion models' application in the same location has been tested in limited studies (Batista et al., 2019; Keller et al., 2021; Li et al., 2017). The lack of studies that focus on global comparison of soil erosion models is even more challenging (Quinton et al., 2010). Moreover, many modelling applications lack adequate model evaluation (e.g., lack of data for validation or evaluation) and can yield highly uncertain soil erosion estimates. In cases where no data for model evaluation is available, a viable alternative may be to adopt multi-model assessments, compare the results and evaluate the degree of consistency of estimates. Such multi-model approaches are used in climate change research (Duan et al., 2019), in which future modelling scenarios are compared (e.g., Coupled Model Intercomparison Project Phase 6 (CMIP6)). We believe that the soil erosion modelling community should also make a similar step towards intercomparison of global multi-models, gaining new insights from the advantages and disadvantages found in the compared models. The topic was also highlighted several times during the Workshop on soil erosion for Europe (JRC, 2022) organised by the EU (European Union) Soil Observatory (EUSO).

Keeping in mind the limited number of soil erosion modelling applications in developing regions (Borrelli et al., 2021), nowadays large-scale soil erosion modelling assessments are often the only resource available for most endangered regions to support policy decisions and the implementation of mitigation strategies. Accordingly, we believe that it would be important to have this knowledge based on multiple soil erosion models, rather than only on USLE-type models. Hence, the Erosion Potential Model (EPM) that also accounts for other erosion processes (e.g., gully erosion or soil slumps) and not just sheet and rill erosion (e.g., USLE-type models) can be an interesting option to estimate global and large-scale soil erosion rates especially because these processes can be important for the erosion-sediment balance at large scales. The main aim of this study is to evaluate the applicability of the Erosion Potential Model (EPM) and its modified version (mEPM) (in combination with selected sediment delivery ratio equations (SDR)) at global scale. Specific objects were to evaluate (i) the sensitivity of the EPM with respect to the input data; (ii) the applicability of EPM and mEPM models in a GIS-environment for global soil erosion assessment and the comparability to USLE type-models; (iii) the performances of the EPM and mEPM models (in combination with SDR) based on the measured suspended sediment yield data from 116 catchment around the globe. To sum up, two most novel aspects of this study are: (i) testing the applicability of two models for global soil erosion assessment and (ii) making important steps towards multi-model soil erosion assessments for further research.

2. Data and methods

2.1. Erosion potential model (EPM) and modified EPM (mEPM)

The original name of the EPM that is currently applied in GIS environment was the Gavrilović method (also named model or equation), named after Slobodan Gavrilović that developed the predictive method back in the 60′s and 70′s based on field research in ex-Yugoslavia (Gavrilović, 1972, 1970, 1962; Gavrilovic, 1988; Gavrilovic et al., 2008). The EPM was developed and calibrated using experimental field data from the Morava River catchment in Serbia, which is characterized by typical continental climate with maximum and minimum temperatures in summer and winter, respectively. According to Micić Ponjiger et al. (2023), a large number of erosion maps of former Yugoslav countries were prepared in the 1980s based on the expert judgment of field data and maps generated via the erosion potential method (EPM) (Gavrilović, 1972) as one of the most widely accepted and applied empirical models in the Balkan region, South, South-East, and Central Europe, as well as the Middle East, North Africa and parts of South America. Consequently, the model was most frequently applied in the Mediterranean region (e.g., countries of the former Yugoslavia, North Africa, Italy, Greece) (Abdullah et al., 2017; Aleksova et al., 2023; Dominici et al., 2020; Dragičević et al., 2016; Efthimiou et al., 2017; El Mouatassime et al., 2019; Gocić et al., 2021, 2020; Karydas et al., 2014; Kostadinov et al., 2017; Mallinis et al., 2009; Manojlović et al., 2018; Nikolic et al., 2019; Ouallali et al., 2020; Spalevic et al., 2020, 2017; Stefanidis and Stathis, 2018), although applications in other climates (e.g., Brazil, Iran, Nepal) can also be found (Chalise et al., 2019; da Silva et al., 2014; Darvishan et al., 2017; de Vente and Poesen, 2005; Lense et al., 2019; Mohammadi et al., 2021; Neto et al., 2022; Sabri et al., 2022; Sakuno et al., 2020; Tavares et al., 2021).

The model is structured as a semi-quantitative method that relates upland soil erosion (i.e., gross erosion) with sediment yield (i.e., net erosion) using the sediment delivery concept (de Vente and Poesen, 2005). The EPM results are averaged (annual) soil erosion rates and the model cannot be used to estimate event-based erosion (Karydas et al., 2014). It should be noted that the EPM model accounts for a variety of erosion processes driven by water such as sheet, rill, interrill, gully erosion as well as some other processes such as soil slumps and bank erosion (Gavrilović, 1970; Gavrilovic, 1988; Gavrilovic et al., 2008). A complete list of processes that were considered during the development of the model was not made available by Gavrilović (1970). However, we may understand that the model does not account for debris material mobilized by large mass movements such as debris flows or deep-seated landslides. Therefore, the method is not limited only to sheet and rill erosion as in case of the USLE-type models (Renard et al., 1997). It should be noted that several additional modules were developed such as a methodology for torrent classification (Gavrilovic et al., 2008). Average annual gross soil erosion (W) [m^3] due to several erosion processes (e.g., sheet, rill, gully, bank erosion) and smaller soil slumps can be calculated as:

$$W = T^{*}P_a{}^{*}\pi^{*}Z^{3/2}{}^{*}A \quad (1)$$

where A is catchment area [km^2], P_a is mean annual precipitation [mm], T is temperature coefficient defined as:

$$T = \sqrt{\frac{T_a}{10} + 0.1} \quad (2)$$

where T_a is mean annual air temperature [°C]. Equation (2) is only valid for T_a above −1 °C. This means that the EPM cannot be applied to polar regions, large parts of the continental climate zones and for high-mountain ranges such as Himalayas where mean annual temperature can also be below −1 °C.

Additionally, Z [-] is erosion coefficient that can be calculated as:

$$Z = Y^{*}X^{*}\left(\rho + \sqrt{S}\right) \quad (3)$$

where Y is a soil erodibility coefficient [-] (Table 1), X is a soil protection coefficient [-] (Table 2), ρ is a coefficient of type and extent of erosion and slumps [-] (Table 3) and S is the mean slope of the investigated catchment [m/m]. Another important aspect is related to the Y, X and ρ coefficients, which in some previous studies were often reported in very simplified way, while the original Gavrilović method (Gavrilović, 1970) used much more detailed description of these coefficients (Table 1, Table 2 and Table 3). Hence, as in most applications of large-scale models, also in this case the original methods that were developed several decades ago are often associated with misuse, simplifications or misunderstanding that can propagate through scientific literature (Chen et al., 2023; Chen and Bezak, 2022; Chen and Huang, 2022), which can lead to greater uncertainty of the results. Moreover, it should be noted Z coefficient can also be used for erosion and torrent categorization (Gavrilovic et al., 2008) (Table 4). This kind of erosion classification can be useful to detect large-scale erosion hotspots around the globe. The workflow of applying the EPM at global scale is shown in Fig. 1.

Moreover, Gavrilović also developed an equation for the estimation of the sediment delivery ratio (*SDR*) that is based on the catchment characteristics (Gavrilović, 1970) and that can be used to calculate net erosion rates taking into account the gross rates (equation (1) and *SDR* (ξ, equation (4) [-] (theoretically the range of the equation is from 0 to 1):

$$\xi = \frac{\sqrt{O^{*}D}}{0.25^{*}(L+10)} \quad (4)$$

where O is catchment perimeter [km], D is mean difference in the elevation of the catchment [km] and L is catchment length [km]. In relation to this equation (i.e., Eq. (4), the definition of the D variable is a bit unclear. Some authors defined it as the average elevation of the catchment (de Vente and Poesen, 2005), others as the difference between maximum and two times minimum elevation of the catchment (Efthimiou et al., 2016) and some as the difference between average and minimum elevation (Lense et al., 2020). Based on the definition available in the original Gavrilović (Gavrilović, 1970), we also believe that the later definition interprets best what was meant in the original publication (Gavrilović, 1970). Hence, this definition was used in this study as well. Moreover, we also found an additional limitation related to Eq. (4) as it can yield *SDR* larger than one for high-gradient streams. For example, if we assume that we have a hypothetical catchment with catchment area of around 50 km^2 of circular shape (i.e., catchment radius is approx. 4 km). In case that slope of the catchment is around 20 %, the calculated *SDR* using Eq. (4) is around one while this can higher if the slope exceeds 20 %. Therefore, Eq. (4) should be applied with caution and should be further tested with an additional catchments dataset that include small, medium, and large catchments. The sediment yield or net erosion rates (G) can be calculated as $G = \xi^{*}W$.

Additionally, we also applied a modified EPM (mEPM) that was developed for the assessment of soil erosion rates in Slovenia after the original version of the EPM (Pintar et al., 1986):

$$W = 20^{*}P_d{}^{*}Z^{3/2}{}^{*}A \quad (5)$$

Table 1
Basic characteristics of Y coefficients according to the original description of the EPM model (Gavrilović, 1970).

Y description – Soil erodibility	*Y* value (coefficient)
Sand, gravel and loose soils	2.0
Loess, tuffs, salt marshes, steppe soils	1.6
Disintegrated limestones and marls	1.2
Serpentines, red sandstones, flysch deposits	1.1
Podzol soils and alike; decomposed shales: mica-schist, gneiss slates, clay slates	1.0
Core limestones and shales, red rocks and humus-silicate soils	0.9
Cambisol and mountain lands	0.8
Vertisol, humogley and wetlands	0.6
Chernozem and alluvial soils of good structure	0.5
Bare compact eruptives (vulcanic origin)	0.25

Table 2
Basic characteristics of X coefficient according to the original description of the EPM model (Gavrilović, 1970).

Additional info	*X* description – soil protection	*X* value (coefficient)
Before implementation of anti-erosion measures	Completely bare, uncultivable land (bare land)	1.0
	Arable land with plowing up or down hill	1.0
	Orchards and vineyards, without ground vegetation	0.7
	Mountain pastures and drylands	0.6
	Meadows, fields and similar agricultural crops	0.4
	Degraded forests and thickets with eroded soil	0.6
	Forests or thickets with good structure and vegetation	0.05
After implementation of anti-erosion measures	Plows with contour plowing (isohypsis direction)	0.6
	Arable land well cared for and protected by mulching	0.5
	Contour strip cultivation with crop rotation (fields)	0.45
	Contour orchards and vineyards	0.3
	Terracing of arable land, terraces and tiers	0.35
	Weeding of bare land and melioration of pastures and drylands	0.3
	Construction of contour trenches of medium density	0.25
	Retardation waterways and micro-accumulations	0.25
	Afforestation with construction of tiers	0.1
	Channel regulation, dam construction and channelization	0.7

Table 3
Basic characteristics ρ coefficient according to the original description of the EPM model (Gavrilović, 1970).

ρ description –type and extent of erosion and slumps	ρ value (coefficient)
Watershed completely under gully erosion and primordial processes (deepening, incision, slumps)	1.0
About 80 % of the watershed is under furrow and gully erosion	0.9
About 50 % of the watershed is under furrow and gully erosion	0.8
The entire watershed is subject to surface erosion: disintegrated debris from embankments, some furrows and gullies, as well as strong karst erosion	0.7
The entire watershed is under surface erosion, but without furrows and gullies (deep processes) and the like	0.6
Land with 50 % of the area covered by surface erosion, while the rest of the watershed is preserved	0.5
Land with 20 % of the area covered by surface erosion, while 80 % of the watershed is preserved	0.3
The soil in the watershed has no visible signs of erosion, but there are minor slips and slides in watercourses	0.2
Watershed without visible signs of erosion, but mostly under arable land	0.15
An area without visible signs of erosion, both in the watershed and in the watercourses, but predominantly under forests and perennial vegetation (meadows, pastures, etc.)	0.1

Table 4
Classification of the erosion classes according to the Z coefficient (adopted after Gavrilovic et al. (2008)).

Erosion category	*Z* coefficient value
Excessive erosion (gullies, rills, rockslides, etc.), category I	$Z > 1$ (mean value of 1.25)
Severe erosion (a bit milder than excessive), category II	$0.71 < Z < 1$ (mean value of 0.85)
Medium erosion, category III	$0.41 < Z < 0.7$ (mean value of 0.55)
Slight erosion, category IV	$0.2 < Z < 0.4$ (mean value of 0.3)
Very slight erosion, category V	$Z < 0.19$ (mean value of 0.1)

where *A* and *Z* parameters are the same as in the case of the original EPM (Eq. (1)) and P_d is maximum daily precipitation [mm]. Hence, the mEPM does not use the air temperature coefficient; the developers of this equation considered the air temperature less important for the erosion processes and the estimated rates in Slovenia (Pintar et al., 1986). Hence, this model was adapted for the soil erosion estimates in smaller typical more torrential catchments located in Alpine zone and temperate continental climates. The mEPM does take into consideration the same processes as the EPM and the result of Eq. (5) are gross erosion rates. The mEPM has been applied for local soil erosion assessments related to water engineering projects in Slovenia (Hrvatin et al., 2019; Petkovšek, 2000). Therefore, it was applied in limited cases. However, the improved version of the EPM is available: the IntErO model that can calculate the soil erosion intensity and runoff at the catchment scale (Chalise et al., 2019; Mohammadi et al., 2021; Neto et al., 2022; Spalevic, 1999; Spalevic et al., 2000; Tavares et al., 2021)

2.2. EPM and modified EPM input data

The original equations of EMP and mEPM were adapted according to the data availability at global scale (Table 5). For the maximum daily precipitation several different products were available (GPCC (i.e., daily data, resolution of 0.5°), PPDIST (i.e., probability distribution dataset, resolution of 0.1°), ERA5 (i.e., daily data, resolution of 0.1°), among others). After testing them, we selected ERA5 based on the best spatial resolution and best representation of the extreme values. Compared to USLE-type models that use rainfall erosivity parameter (e.g., Chen et al., 2023; Lukić et al., 2019; Micić Ponjiger et al., 2023) the EPM and mEPM use simple representation of the water erosion driving force. A second such example is the representation of the landslides or slumps activity that was tested using landslide mobilization rates map (Broeckx et al., 2020) and landslides susceptibility map (Stanley and Kirschbaum, 2017). However, stronger correlation was found between landslides susceptibility map and sediment yield data (Section 2.3) than between landslides mobilization rates map and sediment yield data. Two different gridded data products were generated in relation to ρ coefficient: a first one for erosion (e.g., sheet, rill, gully) and a second one for landslides or slumps. As EPM considers both factors together in ρ coefficient, we used 0.3 wt for landslide or slumps activity and 0.7 wt for erosion activity (i.e., $\rho = 0.7*erosion + 0.3*slumps$). This selection was done since impact of erosion is more represented in the ρ coefficient and it was given higher importance in the original Gavrilović method (Gavrilović, 1970). Additionally, we also checked the dependence between sediment yield (Section 2.3) and erosion and landslide susceptibility map, and the results confirmed the previously mentioned assumption of the relative importance of these two factors. The gridded input data (Table 5) were classified according to the requirements of EPM and mEPM coefficients (Table 1, Table 2 and Table 3) (Supplement). It should be noted that besides information shown in Table 1, Table 2 and Table 3 we also used more general descriptions of the *X, Y* and ρ parameters as shown by Efthimiou et al. (2016) since in some cases it was difficult to find direct connection between descriptions shown in Table 1, Table 2 and Table 3 and data source values (Supplement).

All the calculations were done at 30 arcsec resolution because many products were in this resolution (Table 5). All the input data was resampled to this resolution using B-Spline interpolation included in the SAGA GIS software (SAGA GIS, 2022). After all the input data was resampled to the uniform spatial resolution, the final calculations were conducted using the grid calculator function in SAGA GIS (SAGA GIS,

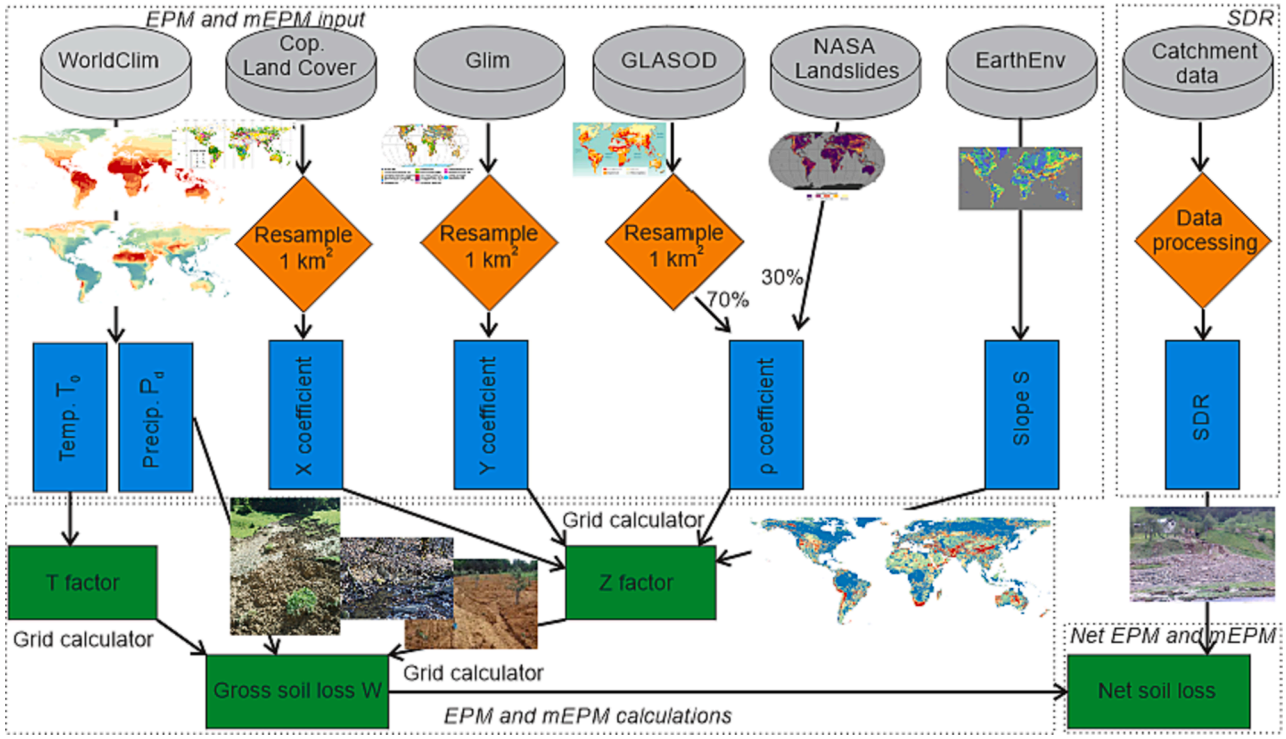

Fig. 1. Workflow of the global application of the EPM with some of the main calculations steps in the GIS system. Input data used is shown in Table 5.

Table 5
Summary of gridded data used as input to the EPM and mEPM.

Parameter [units]	Data source	Spatial resolution or scale	Reference
Mean annual air temperature T_0 [°C]	WorldClim 2.1 (1970–2000)	30 arcsec	(Fick and Hijmans, 2017)
Soil protection coefficient X [/]	Copernicus Land Cover	0.1 km	(Copernicus, 2020)
Soil erodibility coefficient Y [/]	Glim v1.1	1:35 000 000	(Hartmann and Moosdorf, 2012)
Type and extent of erosion and slumps coefficient ρ [/]	GLASOD	1:10 000 000	(ISRIC, 1990)
Type and extent of erosion and slumps coefficient ρ [/]	NASA Landslide Susceptibility map	30 arcsec	(Stanley and Kirschbaum, 2017)
Mean annual precipitation P_a [mm]	WorldClim 2.1 (1970–2000)	30 arcsec	(Fick and Hijmans, 2017)
Maximum daily precipitation P_d [mm]	ERA5 (2015–2020)	0.1°	(Muñoz-Sabater et al., 2021)
Slope [m/m]	EarthEnv	1 km	(Amatulli et al., 2018)
Elevation [km]	EarthEnv	1 km	(Amatulli et al., 2018)

2022). For the input layers that were resampled, we also evaluated the impact of this computational step on the results using the average and standard deviation. In all the cases, the impact was minor. For example, the P_d at 0.1° resolution the mean global value was 59.8 mm with a standard deviation of 45.7 mm while the resampled data at 30 arcsec resolution has the same mean value (i.e., 59.8 mm) and slightly smaller standard deviation (i.e., 45.0 mm). It should be noted that the resampling has an impact at local scale but since the focus of this study was to access the performance at larger (i.e., continental and global) scales, we argue that such impact is less significant than the differences in the original spatial resolution of the selected input data. For the SDR calculations the elevation difference (i.e., D in Eq. (4) was calculated based on the EarthEnv dataset (Amatulli et al., 2018) with a resolution of 10 km. As the proxy for catchment length (i.e., L in Eq. (4) we used the maximum polygon diameter calculated as maximum distance between two polygon part's vertices using SAGA GIS software (SAGA GIS, 2022).

Additionally, for the evaluation of the continental soil erosion rates we used the Hydrologic Derivatives for Modeling and Applications (HDMA) database where catchment boundary data are available for all continents (Verdin, 2017). This dataset contains several raster and vector layers such as flow direction, catchment boundaries or stream network derived from a hybrid digital elevation model using three data sources (Verdin, 2017). The database is suitable for continental-scale modelling (Verdin, 2017). The streams and catchments are defined based on the Pfafstetter codes and using a hierarchical numbering system (Verdin, 2017). In total this dataset contains around 295,000 catchments with average catchment area of around 450 km^2 in Asia and Africa and around 230 km^2 in Europe and South America. The average catchment size in North America and Australia with Oceania was around 290 km^2 and 140 km^2, respectively.

2.3. Sediment yield data

To evaluate the results of our global assessments, we compared the estimates of the EPM and mEPM against a subset (n = 116) of sediment transport data collected by Grill et al. (2019). In total 40, 22, 6, 22, 14 and 12 catchments were in Africa, Asia, Australia with Oceania, Europe, North America, and South America, respectively. This allowed us to cover around approx. 30 million km^2 (i.e., around 20 % of the Earth's surface land) while selected catchments ranged from around 400 km^2 to approximately 3.7 million km^2. We also investigated relationship between EPM and mEPM model performance in relation to the Köppen-Geiger climate classification (Kottek et al., 2006; Peel et al., 2007), as shown in Fig. 2. Moreover, 19, 30, 14, 52 and 1 catchment were in Continental, Tropical, Dry, Temperate and Polar climate zones, respectively (Fig. 2). To better understand the patterns related to under- and over-estimation of the measured sediment yield data by the EPM and mEPM we applied the K-means clustering algorithm implemented in Orange software (Arthur and Vassilvitskii, 2007; Demšar et al., 2013). As target variable bias between observed and modelled sediment yield data for 116 catchments was used and all the relevant data (e.g., latitude, longitude, catchment area, mean discharge, number of dams per catchment, climate zone, max and min elevation) were used as features within the Orange software (Demšar et al., 2013). Number of clusters were set to 4, initialization was done with KMeans++ and 10 re-runs were done with maximum 300 iterations.

2.4. Sensitivity analysis

The sensitivity analysis of the specific EPM and mEPM factors was performed for a range of the coefficients (Table 1, Table 2 and Table 3). More specifically, we used the Sobol sensitivity method (Sobol′, 2001), implemented in R through the Sensitivity package (Iooss et al., 2021). Maximum and minimum ranges of parameters were determined based on the results of a literature review (Table 1, Table 2 and Table 3 and previous papers that applied these models (Abdullah et al., 2017; Dragičević et al., 2016; Efthimiou et al., 2017; Gocić et al., 2020; Kostadinov et al., 2017; Mallinis et al., 2009; Manojlović et al., 2018)). A uniform distribution was used to generate a sequence of parameters for 10,000 model runs using different input parameters for a fixed value of the catchment area A, since it was found that selection of the catchment area does not have a significant impact on the sensitivity analysis results. For example, for the temperature (T) parameter a uniform distribution of values between 0 °C and 35 °C was used. The ranges of parameters for the sensitivity analysis were as follows: 400–4000 mm, 0.1–1, 0.05–1, 0.25–2 and 0.01–0.5 m/m for *Pa, ρ, X, Y* and *S*, respectively. Only first order in the ANOVA decomposition (Iooss et al., 2021) was investigated since the EPM is simple model in terms of mathematical equations applied and computational demands.

3. Results and discussion

3.1. EPM and mEPM results

Fig. 3 shows gross soil erosion rates using the EPM and mEPM with the consideration of the HDMA dataset for the delineation of the catchment boundaries. Hence, the catchment-averaged erosion rates based on the EPM and mEPM result from the mean grid cell values per each catchment are shown in Fig. 3. The EPM yields, on average, higher erosion rates than the mEPM and it is not applicable to several colds regions (i.e., locations where T_a is below −1 °C since Eq. (2) is only valid for T_a above −1 °C) around the globe (Fig. 3). More specifically, the EPM yields higher (1.5–2.5 times) erosion rates compared to the mEPM (Fig. 3). Table 6 shows gross erosion rates using the mEPM that has wider applicability compared to EPM. It should be noted that results for the EPM are not shown because the method cannot be applied to cold regions, consequently there are several regions in Asia, North America, and Europe where averaged continental rates cannot be calculated.

3.2. Sensitivity analysis

For a fixed value of catchment area, it was found that the output of the EPM method is most sensitive to the X and Y coefficients followed by P_a and ρ (Fig. 4). Hence, air temperature and slope have a smaller effect on the results of EPM. The results of this sensitivity analysis are in line with Dragičević et al. (2017) who conducted the sensitivity analysis of EPM in the Dubracina catchment (Croatia); i.e., the highest sensitivity is

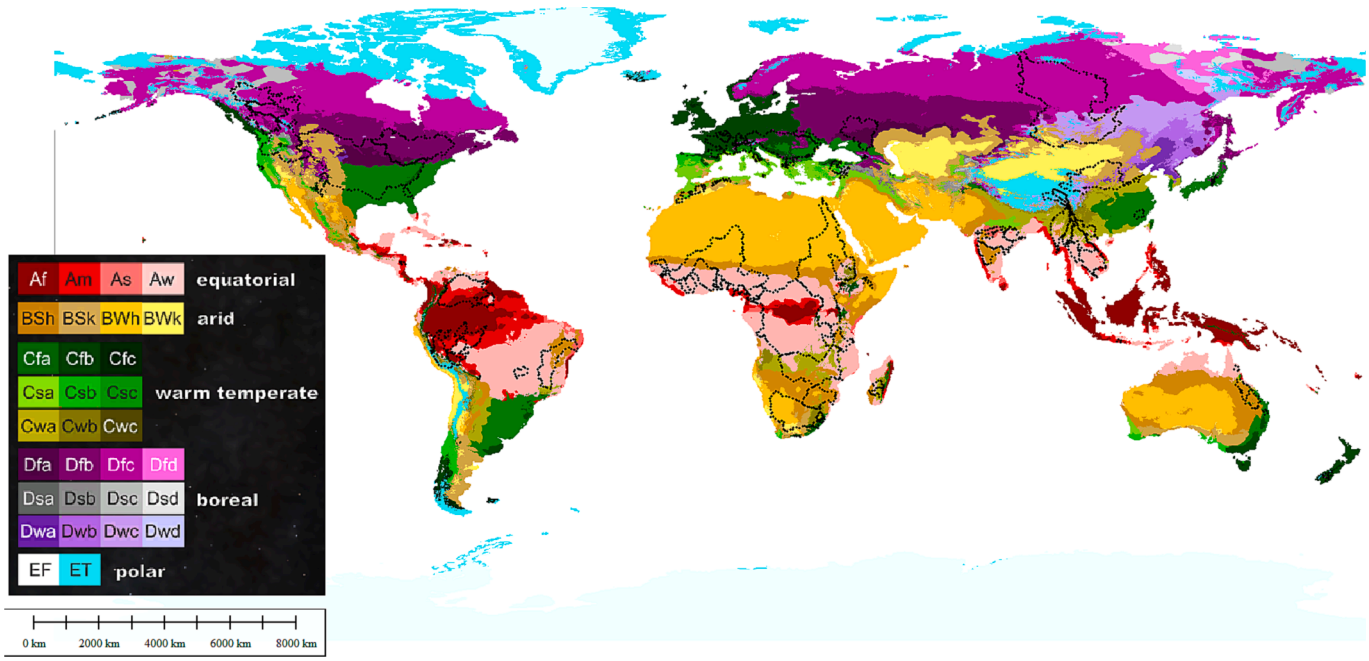

Fig. 2. Location of selected catchments (black polygons) and the Köppen-Geiger climate classification (Kottek et al., 2006; Peel et al., 2007).

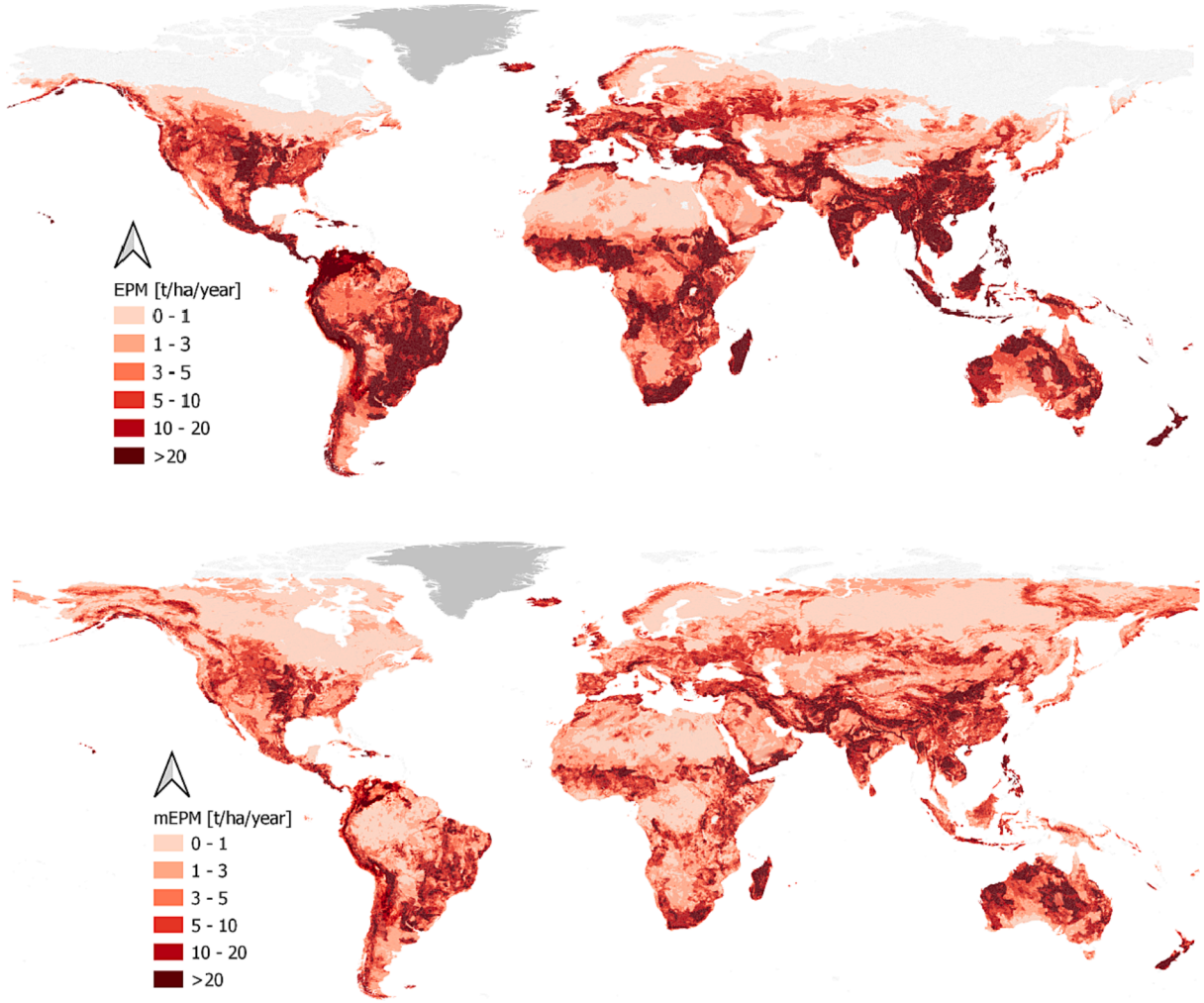

Fig. 3. Global gross soil erosion rates according to the EPM (above) and mEPM (below) with the consideration of the HDMA dataset for the catchment boundaries.

Table 6
Estimated global soil erosion rates using the mEPM.

Continent	Gross mEPM (t ha^{-1} year^{-1})
Asia	6.7
Europe	6.5
Africa	5.3
N America	4.2
S America	7.8
Australia (with Oceania)	10.9
Mean	6.4

for the *X* and *Y* parameters while the impact of air temperature is smaller than precipitation. Renard and Ferreira (1993) indicated the importance of performing the sensitivity evaluation in soil erosion modelling studies. Since most of the global-scale soil erosion modelling applications are based on the USLE-type models it is interesting to compare the sensitivity results of the EPM with the USLE-type models. Only limited number of studies evaluated the sensitivity of the USLE-type models. For example, Odongo et al. (2013) evaluated the sensitivity of the MUSLE (Williams and Berndt, 1977) model using data for a specific catchment in Kenya and found that conceptual factors (i.e., location specific parameters that impact the sediment yield) were contributing to the around two thirds of the variability in the output sediment yield results. Moreover, Estrada-Carmona et al. (2017) and Panagos et al. (2020) evaluated the sensitivity of the RUSLE model and indicated the high importance of the land cover and topography factors. Hence, land cover parameter is particularly important both in EPM and USLE-type models while there is some difference in other parameters such as slope that is less important in the EPM compared to USLE-type models. Parameters with higher sensitivity should be given higher priority in the parameter's estimation process.

3.3. EPM and mEPM evaluation using sediment yield data

For the evaluation of the EPM and mEPM (in combination with SDR) we used the data from 116 catchments (Fig. 2) around the globe as described in section 2.3. Therefore, limitations related to Eq. (2) mean that EPM can only be applied to tropical, arid, and warm temperate climate zones and not to polar regions and high-mountain ranges (Fig. 2, Fig. 3). The mEPM does overcome this issue since it does not consider the air temperature coefficient. This means that the mEPM is more suitable for global scale application compared to the EPM. The EPM also includes methodology for the classification of erosion classes based on the calculated *Z* factor (Fig. S1). For example, Aleksova et al. (2023) used the *Z* factor to evaluate the erosion and landslides risk at the catchment scale. The calculated global *Z* factor could be used to predict large-scale erosion hotspots or for comparison of different catchments and selection of more critical ones where detailed soil erosion studies need to be conducted (Supplement, Fig. S1). The *Z* factor spatial patterns (Fig. S1) are like the ones that are determined by some other soil erosion models although the processes considered are not the same (Borrelli et al., 2017; Naipal et al., 2015; Panagos et al., 2021).

Given the above-mentioned limitations, a comparison between measured annual (long-term averages) suspended sediment yield data and net erosion rates was done only using the mEPM. Therefore, for all selected catchments (Section 2.3) gross and net erosion rates were calculated using the mEPM (Eq. (5). We applied the Eq. (4) to selected 116 catchments (section 2.3) and we found that SDR ranges between 0.1 and 0.8. *SDR* values above 0.6 or 0.7 can be regarded as relatively high (Lu et al., 2006), especially because we selected large catchments for the validation of the EPM and mEPM (i.e., catchment areas ranging from 400 km^2 to 3.7 million km^2 with mean catchment area of 0.25 million km^2). Hence, such large catchments are usually associated with much lower *SDR* values (Lu et al., 2006; Wu et al., 2018). It should be noted that the *SDR* concept is subjected to potential uncertainties due its black-box nature and spatial and temporal lumping (Walling, 1983). However, many improvements related to the *SDR* concept have been made in recent years in respect to the representation of the spatial sediment delivery patterns. This was done with the introduction of the novel concepts such as sediment connectivity (Bracken et al., 2015; Hamel et al., 2017) or spatial representation of the sediment delivery concept (Ali and De Boer, 2010). Therefore, simple equations such as the one

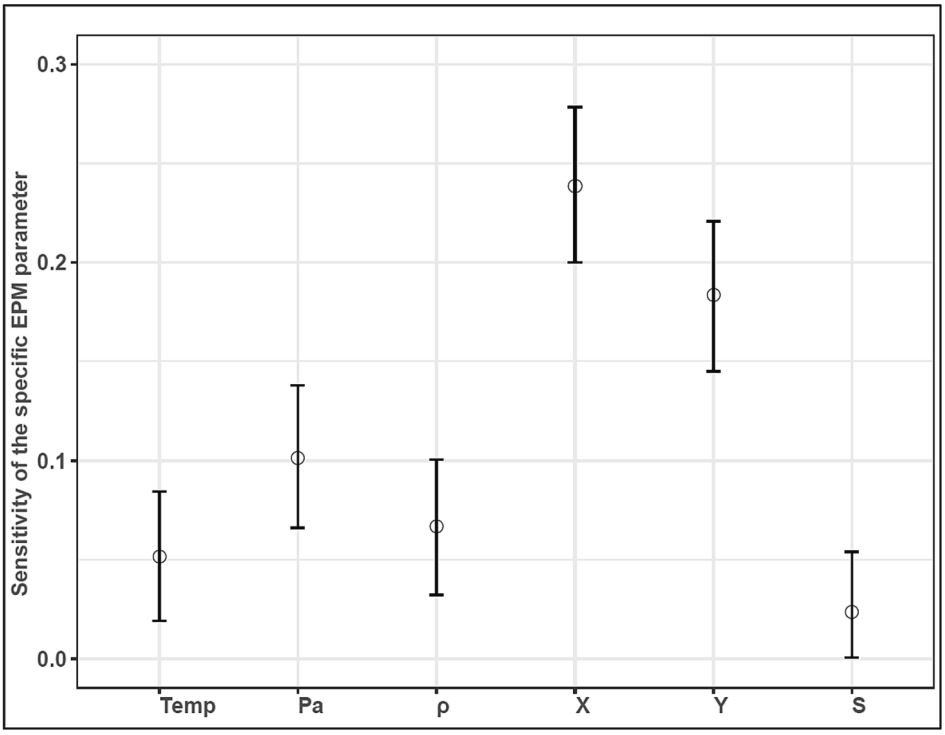

Fig. 4. Results of the sensitivity analysis using Sobol's sensitivity method for the EPM using the methodology described in Section 2.4. The y-axis indicates the sensitivity of the specific EPM parameter and error bars show confidence intervals. Detailed description of parameters is shown in Section 2.1.

proposed by Gavrilović (Gavrilović, 1970) (i.e., Eq. (4)) may encounter some difficulties of parametrization and representativeness. Since the calculated *SDR* values using Eq. (4) were high we additionally tested an equation that does consider some rainfall-runoff processes occurring within the catchment that could have an important impact on the sediment delivery (Didoné et al., 2015; Wu et al., 2018; Williams and Berndt, 1977):

$$SDR = 1.37*10^{-11}*A^{-0.00998}*\left(\frac{R}{L}\right)^{0.363}*CN^{5.44} \quad (6)$$

where A is catchment area [km^2], R is difference in catchment elevation [m], L is length of the catchment [km] and CN is Curve Number (Didoné et al., 2015; Walling, 1983; Wu et al., 2018). The CN parameter is often used in the hydrological rainfall-runoff studies and describes the runoff characteristics of the catchment (Banasik et al., 2014; Zema et al., 2017). It should be noted that average CN parameter (Jaafar et al., 2019) was used in the calculations.

The Pearson correlation coefficient in first case (Fig. 5a) equals to 0.81 (R^2 = 0.66), which implies a strong correlation (Schober and Schwarte, 2018). Moreover, the median bias for the selected 116 catchments is around 10 % which means that mEPM overestimates actual sediment load (Fig. 5, case a). In some catchments, the bias exceeds 100 %, while for others it is close to −100 %. Additionally, applying the EPM instead of the mEPM would yield even larger bias since the EPM yields higher estimates compared to the mEPM (Fig. 3). Applying the Eq. (6) yields slight improvement in terms of agreement between observed suspended sediment rates and net mEPM for the selected 116 catchments (R^2 = 0.68, case b) in Fig. 5) and the calculated SDR values are smaller compared to case b) (i.e., minimum, mean and maximum values equal to 0.08, 0.26 and 0.64, respectively). However, it should be noted that the reported correlation coefficients are depended on the size of catchments used for a comparison. Therefore, an additional comparison was made using observed and modelled specific yield data where catchment area was also considered. In this case, the median bias for the 116 catchments was around 9 % and −8 % for cases a) and

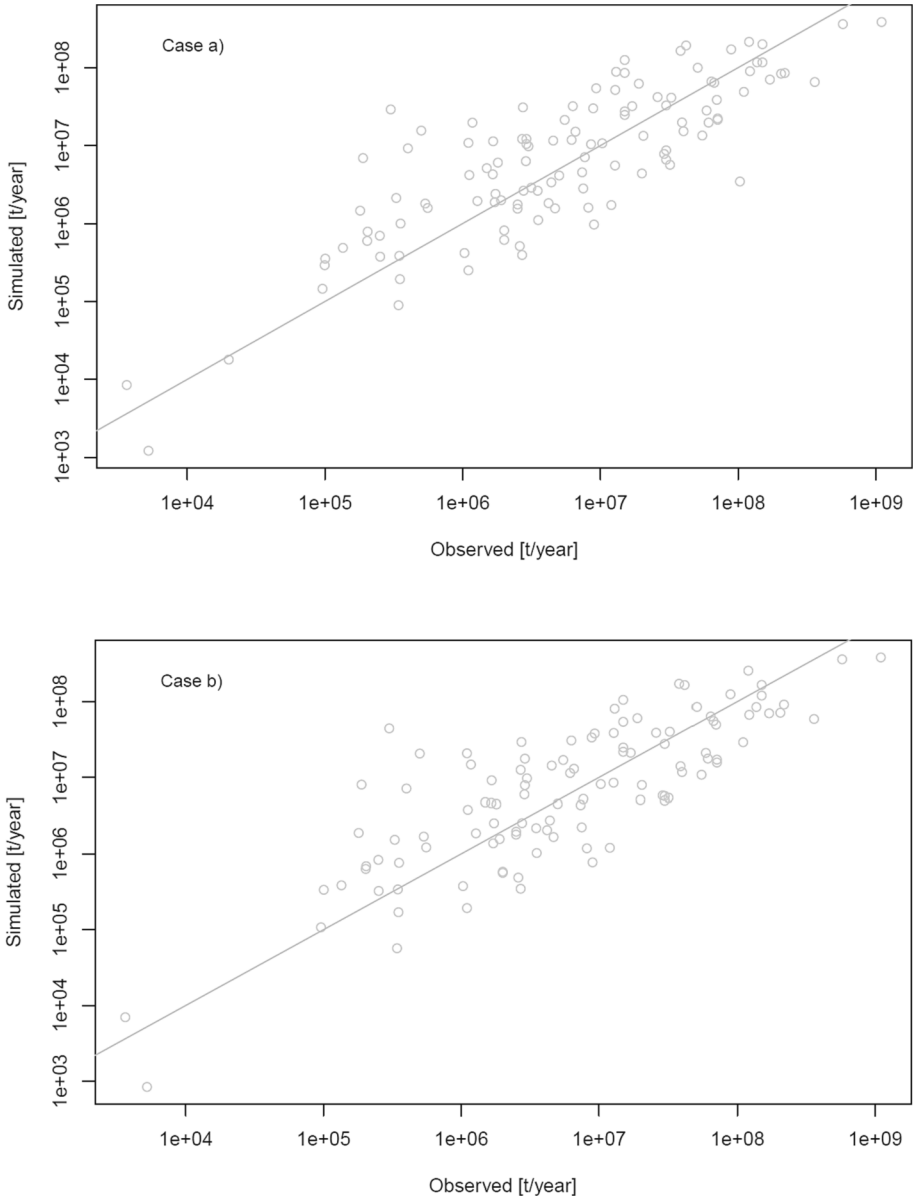

Fig. 5. Comparison between observed suspended sediment load (Section 2.3) and estimated net erosion rates for selected catchments using: a) the Eq. (4) and b) the equation including the CN parameter (Didoné et al., 2015) (Eq. (6). It should be noted that both x and y axis are shown in log-scale. In both cases the y = x line is also shown.

b), respectively. Moreover, for around 1/3 of the selected catchments the bias was more than 100 % or less than −100 %.

Additionally, we also evaluated the agreement between measured suspended sediment load and net erosion rates per climate zones. The best agreement was found for continental and temperate regions. The largest bias was detected for catchments located in the dry climate. Additionally, average bias for catchments located in tropical climate was also relatively large. Hence, besides continental and temperate climates, the EPM and mEPM are also often used in dry regions and some applications in tropical regions can also be found (e.g., Lense et al., 2020). Therefore, applicability of the EPM and mEPM in arid climate should be further evaluated and adjusted using additional validation datasets since erosion processes considered by the EPM and mEPM could not be the most relevant ones in arid climates. However, it should be noted that the number of catchments located in dry climate used in this study was low. Moreover, the applied K-means cluster analysis showed that two big clusters were identified by the algorithm combining most of the catchments. First cluster combined mostly high-elevation catchments with maximum elevation above 2000 m.a.s.l. (and catchment areas less than 10^6 km^2) and the second cluster mostly lower elevation catchments with maximum elevation with less than 2000 m.a.s.l. Additionally, third cluster included mostly either very big catchments or catchments with high maximum elevation. While the last cluster included only a small number of catchments. Hence it is clear that the calculated biases can be partly related to the catchment characteristics meaning that future studies should give more focus on the investigation of the performance of the EPM and mEPM at meso-scale catchments where adequate sediment yield data is available. One example of such dataset is recently compiled EUSEDcollab dataset that could be used in future research to evaluate the EPM more robustly and mEPM at smaller scales (Matthews et al., 2023).

3.4. Evaluation and comparison using other soil erosion models

Additionally, the evaluation of the mEPM was also made at the continental scale using the HDMA dataset (Table 6). The calculated average gross soil erosion rates using the mEPM (Fig. 3) are like the global rates obtained by Naipal et al. (2015) using the adjusted RUSLE model (i.e., mean value of 6.5 ha^{-1} year^{-1} with adjusted *S* and *R*). On the other hand, for Europe much lower sheet and rill erosion rates were obtained by Cerdan et al. (2010) based on upscaling the data obtained from erosion plots (i.e., 1.2 t ha^{-1} year^{-1} for the whole CLC area). Also, the erosion rates calculated by RUSLE2015 (Panagos et al., 2015) (i.e., 2.5 ha^{-1} year^{-1} for the European Union) and PESERA (Kirkby et al., 2008) models for Europe (i.e., 1.5 ha^{-1} year^{-1} for most of the Europe) were much lower compared to mEPM results (Table 6). There is a significant difference in the list of processes that mEPM and other models consider. For example, the USLE-type models account for sheet and rill erosion while PESERA model for rill and inter-rill erosion. On the other hand, EPM and mEPM do account for smaller soil slumps, gully erosion as well as some torrential processes occurring within the river network. Therefore, EPM and mEPM can be regarded as typical equations for description of a wider range of erosion processes and not just sheet and rill erosion. Hence, it can be regarded as an expected result that EPM and mEPM yield higher rates compared to previously mentioned model types. Moreover, some studies like the study conducted by Efthimiou et al. (2016) compared EPM with RUSLE model at catchment scale and both models indicated acceptable performance and were able to identify areas that are most susceptible to erosion and land degradation. However, both tested models underestimated measured sediment yield data and showed some shortcomings.

Moreover, a comparison of the continental erosion rates obtained by Borrelli et al. (2020) indicated that the maximum (i.e., mean of all grid cells per continent) gross erosion rates based on the RUSLE model were obtained for South America followed by Asia, Africa, and Oceania where the average values for the later three were similar (Borrelli et al., 2020). In case of the mEPM (Table 6) the highest gross erosion rates were obtained for Oceania followed by South America and Asia. A bit of discrepancies in this continental comparison can be explained with the fact that the EPM and mEPM also take into consideration other processes such as soil slumps. More specifically, Africa is compared to Europe and other continents less susceptible to landslides according to the landslide's susceptibility map used within this study (Stanley and Kirschbaum, 2017). Moreover, the gross mEPM rates for Europe are like the ones obtained by Borrelli et al. (2023) which considered the concurrent soil erosion processes in Europe (water, wind, gully erosion and erosion due to crop harvesting).

4. Study limitations

It should be noted that there are several limitations related to this study. Firstly, it should be noted that the spatial resolution of input datasets was not the same; therefore, the input data was either aggregated or resampled to the same resolution (30 arcsec). As a result, a coarse gridded map was derived that shows the main large-scale erosion hotspots according to the applied mEPM (Fig. S1). The continental erosion rates shown in Fig. 3 and Table 6 are dependent on the size of the catchments (i.e., HDMA dataset used). However, preliminary analysis for Africa showed that the size of the catchments does not have significant impact on the continental erosion rates budgets. Secondly, the estimation of the EPM coefficients was done using expert knowledge. We did not perform any calibration using sediment data since the EPM parameters should be estimated based on the tabulated descriptions (Gavrilović, 1970). Therefore, in case of local studies where there is also sediment yield data available, EPM and mEPM could be calibrated to obtain more accurate soil erosion estimates. Hence, the main objective of this study was to critically evaluate the usefulness of the EPM and mEPM and estimate global erosion patterns without estimating erosion rates for specific small- and medium-scale catchments. Thirdly, the sediment yield data (section 2.3) was measured in different periods with different methods and different equipment. This means that also long-term sediment yield data represent rough approximation of the actual situation in the selected catchments and that actual sediment transport can vary from year to year. Not to neglect the human impacts on geomorphic processes (Cendrero et al., 2022) that have an impact on land–ocean sediment transfer by the world's rivers (Walling, 2006). Moreover, the derived results should not be used at small spatial scales. At small-scales the EPM and mEPM model parameters should be calibrated using in-situ data. Lastly, there are some limitations related to the EPM and mEPM parameters description and Eq. (4) that were already discussed in the previous sections (i.e., 3.1–3.3).

5. Conclusions

The EPM can be applied globally in regions where mean annual temperature is above −1 °C. Hence, this limits the suitability of this model in polar and parts of the continental climate zones and in high-altitude catchments. The mEPM overcomes this issue but its evaluation using catchment sediment yield data indicated relatively large bias for selected catchments located in arid and tropical regions. Therefore, tested EPM and mEPM have potential limitations in case of global and large-scale assessments, as they have both been developed and tested for upland torrential processes in temperate humid climate. The *Z* factor (erosion coefficient), EPM and mEPM results can be used as an indicator of the large-scale erosion hotspots around the global (Fig. S1). The mEPM yields more realistic gross erosion rates than EPM and could be used for modelling of catchment-based erosion processes. It should be noted that the EPM and mEPM are not able to model the event-based erosion processes or yield seasonal predictions.

The calculated net erosion rates for both EPM and mEPM depend on the selected equation for the estimation of the *SDR*. The equation (i.e., Eq. (4) proposed by Gavrilović (Gavrilović, 1970) yields relatively high

SDR estimates, especially for very large catchments. Moreover, for high-gradient catchments it can also yield a value of *SDR* above 1, which is an unrealistic value and care should be if this equation is to be further used. Including additional information in the estimation of the *SDR* like the hydrological Curve Number (*CN*) parameter can slightly improve the agreement between observed suspended sediment load data and net mEPM rates (Fig. 5). Moreover, applications of simple equations for the *SDR* assessment can yield uncertain results and more sophisticated approaches (i.e., sediment connectivity approach) should be tested in further studies.

An evaluation at global and continental scale revealed that mean global rates obtained using the gross mEPM are higher than rates obtained based on the USLE-type models, which can be regarded as an expected results due to the differences in the considered erosion processes.

To sum up, EPM and mEPM have some potential to be used for large-scale erosion assessments. However, both methods also have several limitations. For example, due the characteristics of both methods the individual parameters (e.g., X or ρ) can have a significant impact on the derived erosion rates. The bias between modelled and observed valuers for some catchments can be large although the median values are less than 10 %. Therefore, additional evaluation should be performed in case of small and medium size catchments where model parameters could be calibrated using the sediment yield data. Finally, the mEPM produced more realistic results (compared to the EPM) which can be further improved in future model application by the soil erosion modelling community. Despite some limitations the results of this study could be used for soil erosion intensity evaluation and land use planning.

Funding

N. Bezak and M. Mikoš would like to acknowledge support from the Slovenian Research Agency through grants J6-4628, N2-0313, J1-2477, J1-3024 and P2-0180 and UNESCO Chair on Water-related Disaster Risk Reduction.

Ethics statements

Not applicable.

Declaration of Competing Interest

The authors declare that they have no known competing financial interests or personal relationships that could have appeared to influence the work reported in this paper.

Data availability

Data will be made available on request.

Acknowledgement

Authors acknowledge the data providers that made the data publicly available. We would like to thank the reviewers and editorial team for their comments and useful suggestions that improved this work.

Appendix A. Supplementary data

Supplementary data to this article can be found online at https://doi.org/10.1016/j.catena.2023.107596.

References

Abdullah, M., Feagin, R., Musawi, L., 2017. The use of spatial empirical models to estimate soil erosion in arid ecosystems. Environ. Monit. Assess. 189, 78. https://doi.org/10.1007/s10661-017-5784-y.

Aleksova, B., Lukić, T., Milevski, I., Spalević, V., Marković, S.B., 2023. Modelling water erosion and mass movements (wet) by using GIS-based multi-hazard susceptibility assessment approaches: a case study: Kratovska Reka catchment (North Macedonia). Atmosphere (Basel) 14. https://doi.org/10.3390/atmos14071139.

Alewell, C., Borrelli, P., Meusburger, K., Panagos, P., 2019. Using the USLE: chances, challenges and limitations of soil erosion modelling. Int. Soil Water Conserv. Res. 7, 203–225. https://doi.org/10.1016/j.iswcr.2019.05.004.

Ali, K.F., De Boer, D.H., 2010. Spatially distributed erosion and sediment yield modeling in the upper Indus River basin. Water Resour. Res. 46 https://doi.org/10.1029/2009WR008762.

Amatulli, G., Domisch, S., Tuanmu, M.-N., Parmentier, B., Ranipeta, A., Malczyk, J., Jetz, W., 2018. Data descriptor: a suite of global, cross-scale topographic variables for environmental and biodiversity modeling. Sci. Data 5. https://doi.org/10.1038/sdata.2018.40.

Amundson, R., Berhe, A.A., Hopmans, J.W., Olson, C., Sztein, A.E., Sparks, D.L., 2015. Soil and human security in the 21st century. Science (80-.) 348, 1261071. https://doi.org/10.1126/science.1261071.

Arthur, D., Vassilvitskii, S., 2007. K-Means++: The Advantages of Careful Seeding. In: Proceedings of the Eighteenth Annual ACM-SIAM Symposium on Discrete Algorithms, SODA '07. Society for Industrial and Applied Mathematics, USA, pp. 1027–1035.

Banasik, K., Rutkowska, A., Kohnová, S., 2014. Retention and curve number variability in a small agricultural catchment: the probabilistic approach. Water (Switzerland) 6, 1118–1133. https://doi.org/10.3390/w6051118.

Batista, P.V.G., Davies, J., Silva, M.L.N., Quinton, J.N., 2019. On the evaluation of soil erosion models: are we doing enough? Earth-Science Rev. 197 https://doi.org/10.1016/j.earscirev.2019.102898.

Batjes, N.H., 1996. Global assessment of land vulnerability to water erosion on a 1/2° by 1/2° grid. L. Degrad. Dev. 7, 353–365. https://doi.org/10.1002/(SICI)1099-145X(199612)7:4<353::AID-LDR239>3.0.CO;2-N.

Bezak, N., Mikoš, M., Borrelli, P., Alewell, C., Alvarez, P., Anache, J.A.A., Baartman, J., Ballabio, C., Biddoccu, M., Cerdà, A., Chalise, D., Chen, S., Chen, W., De Girolamo, A. M., Gessesse, G.D., Deumlich, D., Diodato, N., Efthimiou, N., Erpul, G., Fiener, P., Freppaz, M., Gentile, F., Gericke, A., Haregeweyn, N., Hu, B., Jeanneau, A., Kaffas, K., Kiani-Harchegani, M., Villuendas, I.L., Li, C., Lombardo, L., López-Vicente, M., Lucas-Borja, M.E., Maerker, M., Miao, C., Modugno, S., Möller, M., Naipal, V., Nearing, M., Owusu, S., Panday, D., Patault, E., Patriche, C.V., Poggio, L., Portes, R., Quijano, L., Rahdari, M.R., Renima, M., Ricci, G.F., Rodrigo-Comino, J., Saia, S., Samani, A.N., Schillaci, C., Syrris, V., Kim, H.S., Spinola, D.N., Oliveira, P.T., Teng, H., Thapa, R., Vantas, K., Vieira, D., Yang, J.E., Yin, S., Zema, D.A., Zhao, G., Panagos, P., 2021. Soil erosion modelling: a bibliometric analysis. Environ. Res. 197, 111087 https://doi.org/10.1016/j.envres.2021.111087.

Borrelli, P., Robinson, D.A., Fleischer, L.R., Lugato, E., Ballabio, C., Alewell, C., Meusburger, K., Modugno, S., Schütt, B., Ferro, V., Montanarella, L., Panagos, P., 2017. An assessment of the global impact of 21st century land use change on soil erosion. Nat. Commun. 8 https://doi.org/10.1038/s41467-017-02142-7.

Borrelli, P., Robinson, D.A., Panagos, P., Lugato, E., Yang, J.E., Alewell, C., Wuepper, D., Montanarella, L., Ballabio, C., 2020. Land use and climate change impacts on global soil erosion by water (2015–2070). PNAS 117, 21994–22001. https://doi.org/10.1073/pnas.2001403117.

Borrelli, P., Alewell, C., Alvarez, P., Anache, J.A.A., Baartman, J., Ballabio, C., Bezak, N., Biddoccu, M., Cerdà, A., Chalise, D., Chen, S., Chen, W., De Girolamo, A.M., Gessesse, G.D., Deumlich, D., Diodato, N., Efthimiou, N., Erpul, G., Fiener, P., Freppaz, M., Gentile, F., Gericke, A., Haregeweyn, N., Hu, B., Jeanneau, A., Kaffas, K., Kiani-Harchegani, M., Villuendas, I.L., Li, C., Lombardo, L., López-Vicente, M., Lucas-Borja, M.E., Märker, M., Matthews, F., Miao, C., Mikoš, M., Modugno, S., Möller, M., Naipal, V., Nearing, M., Owusu, S., Panday, D., Patault, E., Patriche, C.V., Poggio, L., Portes, R., Quijano, L., Rahdari, M.R., Renima, M., Ricci, G.F., Rodrigo-Comino, J., Saia, S., Samani, A.N., Schillaci, C., Syrris, V., Kim, H.S., Spinola, D.N., Oliveira, P.T., Teng, H., Thapa, R., Vantas, K., Vieira, D., Yang, J.E., Yin, S., Zema, D.A., Zhao, G., Panagos, P., 2021. Soil erosion modelling: a global review and statistical analysis. Sci. Total Environ. 146494 https://doi.org/10.1016/j.scitotenv.2021.146494.

Borrelli, P., Ballabio, C., Yang, J.E., Robinson, D.A., Panagos, P., 2022. GloSEM: high-resolution global estimates of present and future soil displacement in croplands by water erosion. Sci. Data 9, 406. https://doi.org/10.1038/s41597-022-01489-x.

Borrelli, P., Panagos, P., Alewell, C., Ballabio, C., de Oliveira Fagundes, H., Haregeweyn, N., Lugato, E., Maerker, M., Poesen, J., Vanmaercke, M., Robinson, D. A., 2023. Policy implications of multiple concurrent soil erosion processes in European farmland. Nat. Sustain. 6, 103–112. https://doi.org/10.1038/s41893-022-00988-4.

Bracken, L.J., Turnbull, L., Wainwright, J., Bogaart, P., 2015. Sediment connectivity: a framework for understanding sediment transfer at multiple scales. Earth Surf. Process. Landforms 40, 177–188. https://doi.org/10.1002/esp.3635.

Broeckx, J., Rossi, M., Lijnen, K., Campforts, B., Poesen, J., Vanmaercke, M., 2020. Landslide mobilization rates: a global analysis and model. Earth-Science Rev. 201, 102972 https://doi.org/10.1016/j.earscirev.2019.102972.

Cendrero, A., Remondo, J., Beylich, A.A., Cienciala, P., Forte, L.M., Golosov, V.N., Gusarov, A.V., Kijowska-Strugała, M., Laute, K., Li, D., Navas, A., Soldati, M., Vergari, F., Zwoliński, Z., Dixon, J.C., Knight, J., Nadal-Romero, E., Płaczkowska, E., 2022. Denudation and geomorphic change in the Anthropocene; a global overview. Earth-Science Rev. 233, 104186 https://doi.org/10.1016/j.earscirev.2022.104186.

Cerdan, O., Govers, G., Le Bissonnais, Y., Van Oost, K., Poesen, J., Saby, N., Gobin, A., Vacca, A., Quinton, J., Auerswald, K., Roxo, M.J., Dostal, T., 2010. Rates and spatial variations of soil erosion in Europe: a study based on erosion plot data. Geomorphology 122, 167–177. https://doi.org/10.1016/j.geomorph.2010.06.011.

Chalise, D., Kumar, L., Spalevic, V., Skataric, G., 2019. Estimation of sediment yield and maximum outflow using the IntErO model in the Sarada River Basin of Nepal. Water (Switzerland) 11. https://doi.org/10.3390/w11050952.

Chen, W., Bezak, N., 2022. Comment on "Towards improved USLE-based soil erosion modelling in India: a review of prevalent pitfalls and implementation of exemplar methods" by Majhi et al. (2021). Earth-Sci. Rev. 221, 103786. Earth-Science Rev. 104095. 10.1016/j.earscirev.2022.104095.
Chen, W., Huang, Y.-C., 2022. Comment on "Multi-fractal characteristics of reconstructed landform and its relationship with soil erosion at a large opencast coal-mine in the loess area of China" by Shi et al. (2021). Geomorphology. 10.1016/j.geomorph.2022.108188.
Chen, W., Huang, Y.-C., Lebar, K., Bezak, N., 2023. A systematic review of the incorrect use of an empirical equation for the estimation of the rainfall erosivity around the globe. Earth-Sci. Rev. 238, 104339 https://doi.org/10.1016/j.earscirev.2023.104339.
Copernicus, 2020. Global Land's first global 100 m land cover map [WWW Document]. https://land.copernicus.eu/global/content/annual-100m-global-land-cover-maps-available.
da Silva, R.M., Santos, C.A.G., Silva, A.M., 2014. Predicting soil erosion and sediment yield in the Tapacurá catchment. Brazil. J. Urban Environ. Eng. 8, 75–82. https://doi.org/10.4090/juee.2014.v8n1.075082.
Darvishan, A.K., Behzadfar, M., Spalevic, V., Kalonde, P., Ouallali, A., El Mouatassime, S., 2017. Calculation of sediment yield in the S2–1 watershed of the Shirindareh River Basin. Iran. Agric. for. 63, 23–32.
de Vente, J., Poesen, J., 2005. Predicting soil erosion and sediment yield at the basin scale: scale issues and semi-quantitative models. Earth-Science Rev. 71, 95–125. https://doi.org/10.1016/j.earscirev.2005.02.002.
Demšar, J., Curk, T., Erjavec, A., Gorup, Č., Hočevar, T., Milutinovič, M., Možina, M., Polajnar, M., Toplak, M., Starič, A., Štajdohar, M., Umek, L., Žagar, L., Žbontar, J., Žitnik, M., Zupan, B., 2013. Orange: data mining toolbox in python. J. Mach. Learn. Res. 14, 2349–2353.
Didoné, E.J., Minella, J.P.G., Merten, G.H., 2015. Quantifying soil erosion and sediment yield in a catchment in southern Brazil and implications for land conservation. J. Soil. Sediment. 15, 2334–2346. https://doi.org/10.1007/s11368-015-1160-0.
Dominici, R., Larosa, S., Viscomi, A., Mao, L., De Rosa, R., Cianflone, G., 2020. Yield erosion sediment (YES): a PyQGIS plug-in for the sediments production calculation based on the erosion potential method. Geosciences 10. https://doi.org/10.3390/geosciences10080324.
Dragičević, N., Karleuša, B., Ožanić, N., 2016. A review of the Gavrilović method (erosion potential method) application. Gradjevinar 68, 715–725. https://doi.org/10.14256/JCE.1602.2016.
Dragičević, N., Karleuša, B., Ožanić, N., 2017. Erosion potential method (Gavrilović Method) sensitivity analysis. Soil Water Res. 12, 51–59. https://doi.org/10.17221/27/2016-SWR.
Duan, H., Zhang, G., Wang, S., Fan, Y., 2019. Robust climate change research: A review on multi-model analysis. Environ. Res. Lett. 14 https://doi.org/10.1088/1748-9326/aaf8f9.
Efthimiou, N., Lykoudi, E., Panagoulia, D., Karavitis, C., 2016. Assessment of soil susceptibility to erosion using the epm and rusle models: the case of venetikos river catchment. Glob. Nest J. 18, 164–179. https://doi.org/10.30955/gnj.001847.
Efthimiou, N., Lykoudi, E., Karavitis, C., 2017. Comparative analysis of sediment yield estimations using different empirical soil erosion models. Hydrol. Sci. J. 62, 2674–2694. https://doi.org/10.1080/02626667.2017.1404068.
El Mouatassime, S., Boukdir, A., Karaoui, I., Skataric, G., Nacka, M., Khaledi Darvishan, A., Sestras, P., Spalevic, V., 2019. Modelling of soil erosion processes and runoff for sustainable watershed management: case study oued el abid watershed, Morocco. Agric. for. 65, 241–250. https://doi.org/10.17707/AgricultForest.65.4.22.
Estrada-Carmona, N., Harper, E.B., DeClerck, F., Fremier, A.K., 2017. Quantifying model uncertainty to improve watershed-level ecosystem service quantification: a global sensitivity analysis of the RUSLE. Int. J. Biodivers. Sci. Ecosyst. Serv. Manag. 13, 40–50. https://doi.org/10.1080/21513732.2016.1237383.
FAO, 2019. Global Symposium on Soil Erosion (GSER 2019): Symposium working documents. Italy, Rome.
Fick, S.E., Hijmans, R.J., 2017. WorldClim 2: new 1-km spatial resolution climate surfaces for global land areas. Int. J. Climatol. 37, 4302–4315. https://doi.org/10.1002/joc.5086.
Gavrilović, S., 1962. Proračun srednje-godišnje količine nanosa prema potencijalu erozije. Glas. Šumarskog Fak. 26, 151–168.
Gavrilovic, Z., Stefanovic, M., Milovanovic, I., Cotric, J., Milojevic, M., 2008. Torrent Classification – Base of Rational Management of Erosive Regions. In: XXIVth Conference of the Danubian Countries. Bled, Slovenia, pp. 1–9. 10.1088/1755-1307/4/1/012039.
Gavrilović, S., 1970. Savremeni načini proračunavanja bujičnih nanosa i izrada karata erozije. In: Seminar Erozija, Bujični Tokovi i Rečni Nanos. Belgrade, pp. 85–100.
Gavrilović, S., 1972. Inženjering o bujičnim tokovima i eroziji. Belgrade: Republic water fund of the SR Serbia, Belgrade: Water management organization "Belgrade": Institute for erosion, melioration and water management of torrential streams at the Faculty of Forestry, Belgrade.
Gavrilovic, Z., 1988. The use of an empirical method (Erosion Potential Method) for calculating sediment production and transportation in unstudied or torrential streams. In: Proceedings of the International Conference OnRiver Regime. Wallingford, UK.
Gocić, M., Dragićević, S., Radivojević, A., Martić Bursać, N., Stričević, L., Đorđević, M., 2020. Changes in soil erosion intensity caused by land use and demographic changes in the Jablanica River basin, Serbia. Agriculture 10. https://doi.org/10.3390/agriculture10080345.
Gocić, M., Dragićević, S., Živanović, S., Ivanović, R., Martić Bursać, N., Stričević, L., Radivojević, Ž., J., a.,, 2021. Assessment of soil erosion intensity in the Kutinska river basin in the period 1971–2016. Fresenius Environ. Bull. 30, 10890–10898.
Grill, G., Lehner, B., Thieme, M., Geenen, B., Tickner, D., Antonelli, F., Babu, S., Borrelli, P., Cheng, L., Crochetiere, H., Ehalt Macedo, H., Filgueiras, R., Goichot, M., Higgins, J., Hogan, Z., Lip, B., McClain, M.E., Meng, J., Mulligan, M., Nilsson, C., Olden, J.D., Opperman, J.J., Petry, P., Reidy Liermann, C., Sáenz, L., Salinas-Rodríguez, S., Schelle, P., Schmitt, R.J.P., Snider, J., Tan, F., Tockner, K., Valdujo, P. H., van Soesbergen, A., Zarfl, C., 2019. Mapping the world's free-flowing rivers. Nature 569, 215–221. https://doi.org/10.1038/s41586-019-1111-9.
Hamel, P., Falinski, K., Sharp, R., Auerbach, D.A., Sánchez-Canales, M., Dennedy-Frank, P.J., 2017. Sediment delivery modeling in practice: Comparing the effects of watershed characteristics and data resolution across hydroclimatic regions. Sci. Total Environ. 580, 1381–1388. https://doi.org/10.1016/j.scitotenv.2016.12.103.
Hartmann, J., Moosdorf, N., 2012. The new global lithological map database GLiM: a representation of rock properties at the Earth surface. Geochem., Geophys. Geosystems 13. https://doi.org/10.1029/2012GC004370.
Hrvatin, M., Ciglič, R., Lóczy, D., Zorn, M., 2019. Determination of erosion in low hills of Northeast Slovenia with gavrilović equation; [Določanje erozije v gričevjih severovzhodne slovenije z gavrilovićevo enačbo]. Geogr. Vestn. 91, 105–124. https://doi.org/10.3986/GV91206.
Iooss, B., Veiga, S. Da, Janon, A., Pujol, G., with contributions from Baptiste Broto, Boumhaout, K., Delage, T., Amri, R. El, Fruth, J., Gilquin, L., Guillaume, J., Herin, M., Idrissi, M. Il, Le Gratiet, L., Lemaitre, P., Marrel, A., Meynaoui, A., Nelson, B.L., Monari, F., Oomen, R., Rakovec, O., Ramos, B., Roustant, O., Song, E., Staum, J., Sueur, R., Touati, T., Verges, V., Weber, F., 2021. Sensitivity: Global Sensitivity Analysis of Model Outputs.
Isric, 1990. GLASOD [WWW Document]. Glob. Assess, Human-induced Soil Degrad https://data.isric.org/geonetwork/srv/eng/catalog.search#/metadata/9e84c15e-cb46-45e2-9126-1ca38bd5cd22.
Jaafar, H.H., Ahmad, F.A., El Beyrouthy, N., 2019. GCN250, new global gridded curve numbers for hydrologic modeling and design. Sci. Data 6, 145. https://doi.org/10.1038/s41597-019-0155-x.
Jrc, 2022. Soil Erosion Workshop [WWW Document]. Work, Proc https://esdac.jrc.ec.europa.eu/public_path/EUSO/proceedings_ALL.pdf.
Karydas, C.G., Panagos, P., Gitas, I.Z., 2014. A classification of water erosion models according to their geospatial characteristics. Int. J. Digit. Earth 7, 229–250. https://doi.org/10.1080/17538947.2012.671380.
Keller, B., Centeri, C., Szabó, J.A., Szalai, Z., Jakab, G., 2021. Comparison of the applicability of different soil erosion models to predict soil erodibility factor and event soil losses on loess slopes in hungary. Water 13. https://doi.org/10.3390/w13243517.
Kirkby, M.J., Imeson, A.C., Bergkamp, G., Cammeraat, L.H., 1996. Scaling up processes and models from the field plot to the watershed and regional areas. J. Soil Water Conserv. 51, 391–396.
Kirkby, M.J., Irvine, B.J., Jones, R.J.A., Govers, G., Boer, M., Cerdan, O., Daroussin, J., Gobin, A., Grimm, M., Le Bissonnais, Y., Puigdefabregas, J., Van Lynden, G., 2008. The PESERA coarse scale erosion model for Europe. I. - model rationale and implementation. Eur. J. Soil Sci. 59, 1293–1306. https://doi.org/10.1111/j.1365-2389.2008.01072.x.
Kostadinov, S., Dragićević, S., Stefanović, T., Novković, I., Petrović, A.M., 2017. Torrential flood prevention in the Kolubara river basin. J. Mt. Sci. 14, 2230–2245. https://doi.org/10.1007/s11629-017-4575-9.
Kottek, M., Grieser, J., Beck, C., Rudolf, B., Rubel, F., 2006. World map of the Köppen-Geiger climate classification updated. Meteorol. Zeitschrift 15, 259–263. https://doi.org/10.1127/0941-2948/2006/0130.
Laflen, J.M., Lane, L.J., Foster, G.R., 1991. WEPP: a new generation of erosion prediction technology. J. Soil & Water Conserv. 46, 34–38.
Lense, G.H.E., Parreiras, T.C., Moreira, R.S., Avanzi, J.C., Mincato, R.L., 2019. Estimates of soil losses by the erosion potential method in tropical latosols; [Estimativas de perdas de solo pelo método de erosão potencial em latossolos tropicais]. Cienc. e Agrotecnol. 43 https://doi.org/10.1590/1413-7054201943012719.
Lense, G.H.E., Moreira, R.S., Parreiras, T.C., Santana, D.B., Bolelli, T.M., Mincato, R.L., 2020. Water erosion modeling by the erosion potential method and the revised universal soil loss equation: A comparative analysis | Modelagem da erosão hídrica pelo método de erosão potencial e pela equação universal de perda de solo revisada: Uma análise compa. Rev. Ambient. e Agua 15, 1–11. https://doi.org/10.4136/ambi-agua.2501.
Li, P., Mu, X., Holden, J., Wu, Y., Irvine, B., Wang, F., Gao, P., Zhao, G., Sun, W., 2017. Comparison of soil erosion models used to study the Chinese Loess Plateau. Earth-Sci. Rev. 170, 17–30. https://doi.org/10.1016/j.earscirev.2017.05.005.
Lu, H., Moran, C.J., Prosser, I.P., 2006. Modelling sediment delivery ratio over the Murray Darling Basin. Environ. Model. Softw. 21, 1297–1308. https://doi.org/10.1016/j.envsoft.2005.04.021.
Lukić, T., Lukić, A., Basarin, B., Ponjiger, T.M., Blagojević, D., Mesaroš, M., Milanović, M., Gavrilov, M., Pavić, D., Zorn, M., Morar, C., Janićević, S., 2019. Rainfall erosivity and extreme precipitation in the Pannonian basin. Open Geosci. 11, 664–681. https://doi.org/10.1515/geo-2019-0053.
Mallinis, G., Maris, F., Kalinderis, I., Koutsias, N., 2009. Assessment of post-fire soil erosion risk in fire-affected watersheds using remote sensing and GIS. Gisci. Remote Sens. 46, 388–410. https://doi.org/10.2747/1548-1603.46.4.388.
Manojlović, S., Antić, M., Šantić, D., Sibinović, M., Carević, I., Srejić, T., 2018. Anthropogenic impact on erosion intensity: case study of rural areas of pirot and dimitrovgrad municipalities. Serbia. Sustainability 10. https://doi.org/10.3390/su10030826.
Matthews, F., Verstraeten, G., Borrelli, P., Vanmaercke, M., Poesen, J., Steegen, A., Degré, A., Rodríguez, B.C., Bielders, C., Franke, C., Alary, C., Zumr, D., Patault, E., Nadal-Romero, E., Smolska, E., Licciardello, F., Swerts, G., Thodsen, H., Casalí, J., Eslava, J., Richet, J.-B., Ouvry, J.-F., Farguell, J., Święchowicz, J., Nunes, J.P.,

Pak, L.T., Liakos, L., Campo-Bescós, M.A., Żelazny, M., Delaporte, M., Pineux, N., Henin, N., Bezak, N., Lana-Renault, N., Tzoraki, O., Giménez, R., Li, T., Zuazo, V.H. D., Bagarello, V., Pampalone, V., Ferro, V., Úbeda, X., Panagos, P., 2023. EUSEDcollab: a network of data from European catchments to monitor net soil erosion by water. Sci. Data 10, 515. https://doi.org/10.1038/s41597-023-02393-8.

Micić Ponjiger, T., Lukić, T., Wilby, R.L., Marković, S.B., Valjarević, A., Dragićević, S., Gavrilov, M.B., Ponjiger, I., Durlević, U., Milanović, M.M., Basarin, B., Mlađan, D., Mitrović, N., Grama, V., Morar, C., 2023. Evaluation of rainfall erosivity in the western balkans by mapping and clustering ERA5 reanalysis data. Atmosphere (Basel) 14. https://doi.org/10.3390/atmos14010104.

Mohammadi, M., Darvishan, A.K., Spalevic, V., Dudic, B., Billi, P., 2021. Analysis of the impact of land use changes on soil erosion intensity and sediment yield using the intero model in the talar watershed of iran. Water (Switzerland) 13. https://doi.org/10.3390/w13060881.

Montgomery, D.R., 2007. Soil erosion and agricultural sustainability. Proc. Natl. Acad. Sci. 104, 13268–13272. https://doi.org/10.1073/pnas.0611508104.

Muñoz-Sabater, J., Dutra, E., Agustí-Panareda, A., Albergel, C., Arduini, G., Balsamo, G., Boussetta, S., Choulga, M., Harrigan, S., Hersbach, H., Martens, B., Miralles, D.G., Piles, M., Rodríguez-Fernández, N.J., Zsoter, E., Buontempo, C., Thépaut, J.N., 2021. ERA5-Land: a state-of-the-art global reanalysis dataset for land applications. Earth Syst. Sci. Data 13, 4349–4383. https://doi.org/10.5194/essd-13-4349-2021.

Naipal, V., Reick, C., Pongratz, J., Van Oost, K., 2015. Improving the global applicability of the RUSLE model - adjustment of the topographical and rainfall erosivity factors. Geosci. Model Dev. 8, 2893–2913. https://doi.org/10.5194/gmd-8-2893-2015.

Nearing, M.A., Wei, H., Stone, J.J., Pierson, F.B., Spaeth, K.E., Weltz, M.A., Flanagan, D. C., Hernandez, M., 2011. A rangeland hydrology and erosion model. Trans. ASABE 54, 901–908.

Neto, M.R.R., Musselli, D.G., Lense, G.H.E., Servidoni, L.E., Stefanidis, S., Spalevic, V., Mincato, R.L., 2022. Soil loss modelling by the IntErO model-erosion potential method in the Machado River Basin, Minas Gerais, Brazil. Agric. For. 68, 7–21. https://doi.org/10.17707/AgricultForest.68.2.01.

Nikolic, G., Spalevic, V., Curovic, M., Khaledi Darvishan, A., Skataric, G., Pajic, M., Kavian, A., Tanaskovik, V., 2019. Variability of soil erosion intensity due to vegetation cover changes: case study of Orahovacka Rijeka, montenegro. Not. Bot. Horti Agrobot. Cluj-Napoca 47, 237–248. https://doi.org/10.15835/nbha47111310.

Odongo, V.O., Onyando, J.O., Mutua, B.M., van Oel, P.R., Becht, R., 2013. Sensitivity analysis and calibration of the Modified Universal Soil Loss Equation (MUSLE) for the upper Malewa Catchment, Kenya. Int. J. Sediment. Res. 28, 368–383. https://doi.org/10.1016/S1001-6279(13)60047-5.

Ouallali, A., Aassoumi, H., Moukhchane, M., Moumou, A., Houssni, M., Spalevic, V., Keesstra, S., 2020. Sediment mobilization study on Cretaceous, Tertiary and Quaternary lithological formations of an external Rif catchment, Morocco. Hydrol. Sci. J. 65, 1568–1582. https://doi.org/10.1080/02626667.2020.1755435.

Panagos, P., Borrelli, P., Poesen, J., Ballabio, C., Lugato, E., Meusburger, K., Montanarella, L., Alewell, C., 2015. The new assessment of soil loss by water erosion in Europe. Environ. Sci. Policy 54, 438–447. https://doi.org/10.1016/j.envsci.2015.08.012.

Panagos, P., Ballabio, C., Poesen, J., Lugato, E., Scarpa, S., Montanarella, L., Borrelli, P., 2020. A soil erosion indicator for supporting agricultural, environmental and climate policies in the European Union. Remote Sens. 12 https://doi.org/10.3390/rs12091365.

Panagos, P., Ballabio, C., Himics, M., Scarpa, S., Matthews, F., Bogonos, M., Poesen, J., Borrelli, P., 2021. Projections of soil loss by water erosion in Europe by 2050. Environ. Sci. Policy 124, 380–392. https://doi.org/10.1016/j.envsci.2021.07.012.

Panagos, P., Borrelli, P., Matthews, F., Liakos, L., Bezak, N., Diodato, N., Ballabio, C., 2022. Global rainfall erosivity projections for 2050 and 2070. J. Hydrol. 610, 127865 https://doi.org/10.1016/j.jhydrol.2022.127865.

Peel, M.C., Finlayson, B.L., McMahon, T.A., 2007. Updated world map of the Köppen-Geiger climate classification. Hydrol. Earth Syst. Sci. 11, 1633–1644. https://doi.org/10.5194/hess-11-1633-2007.

Petkovšek, G., 2000. Therefore, it was appliedin very limited cases. Acta Hydrotech. 18, 41–60.

Pintar, J., Mikop, M., Verbovšek, V., 1986. Elementi okolju prilagojenega urejanja vodotokov – alternativa utesnjevanju živih naravnih procesov v toge objekte. In: Zbornik 2. Kongresa o Vodah Jugoslavije. Ljubljana, pp. 800–814.

Quinton, J.N., Govers, G., Van Oost, K., Bardgett, R.D., 2010. The impact of agricultural soil erosion on biogeochemical cycling. Nat. Geosci. 3, 311–314. https://doi.org/10.1038/ngeo838.

Renard, K.G., Foster, G.R., Weesies, G.A., McCool, D.K., Yoder, D.C., 1997. Predicting Soil Erosion byWater: A Guide to Conservation Planning with the Revised Universal Soil Loss Equation (RUSLE) (Agricultural Handbook 703).

Renard, K.G., Ferreira, V.A., 1993. RUSLE model description and database sensitivity. J. Environ. Qual. 22, 458–466. https://doi.org/10.2134/jeq1993.00472425002200030009x.

Sabri, E., Spalevic, V., Boukdir, A., Karaoui, I., Ouallali, A., Mincato, R.L., Sestras, P., 2022. Estimation of soil losses and reservoir sedimentation: a case study in Tillouguite Sub-Basin (high Atlas-Morocco). Agric. For. 68, 207–220. https://doi.org/10.17707/AgricultForest.68.2.15.

SAGA GIS, 2022. SAGA GIS.

Sakuno, N.R.R., Guiçardi, A.C.F., Spalevic, V., Avanzi, J.C., Silva, M.L.N., Mincato, R.L., 2020. Adaptation and application of the erosion potential method for tropical soils. Rev. Cienc. Agron. 51, 1–10. https://doi.org/10.5935/1806-6690.20200004.

Schober, P., Schwarte, L.A., 2018. Correlation coefficients: appropriate use and interpretation. Anesth. Analg. 126, 1763–1768. https://doi.org/10.1213/ANE.0000000000002864.

Sobol′, I.M., 2001. Global sensitivity indices for nonlinear mathematical models and their Monte Carlo estimates. Math. Comput. Simul 55, 271–280. https://doi.org/10.1016/S0378-4754(00)00270-6.

Spalevic, V., 1999. Application of computer-graphic methods in the studies of draining out and intensities of ground erosion in the Berane valley. University of Belgrade.

Spalevic, V., Dlabac, A., Spalevic, B., Fustic, B., Popovic, V., 2000. Application of computer - graphic methods in the research of runoff and intensity of ground erosion - I program "River basins". Agriculture and Forestry.

Spalevic, V., Lakicevic, M., Radanovic, D., Billi, P., Barovic, G., Vujacic, D., Sestras, P., Khaledi Darvishan, A., 2017. Ecological-Economic (Eco-Eco) modelling in the river basins of Mountainous Regions: impact of land cover changes on sediment yield in the Velicka Rijeka, Montenegro. Not. Bot. Horti Agrobot. Cluj-Napoca 45, 602–610. https://doi.org/10.15835/nbha45210695.

Spalevic, V., Barovic, G., Vujacic, D., Curovic, M., Behzadfar, M., Djurovic, N., Dudic, B., Billi, P., 2020. The impact of land use changes on soil erosion in the river basin of miocki potok, montenegro. Water (switzerland) 12, 1–28. https://doi.org/10.3390/w12112973.

Stanley, T., Kirschbaum, D.B., 2017. A heuristic approach to global landslide susceptibility mapping. Nat. Hazards 87, 145–164. https://doi.org/10.1007/s11069-017-2757-y.

Stefanidis, S., Stathis, D., 2018. Effect of climate change on soil erosion in a mountainous mediterranean catchment (Central Pindus, Greece). Water (Switzerland) 10. https://doi.org/10.3390/w10101469.

Tavares, A.S., Uagoda, R.E.S., Spalevic, V., Mincato, R.L., 2021. Analysis of the erosion potential and sediment yield using the intero model in an experimental watershed dominated by karst in brazil. Agric. for. 67, 153–162. https://doi.org/10.17707/AgricultForest.67.2.11.

USDA, 2019. Conservation practices have decreased soil erosion on cultivated cropland over time [WWW Document]. https://www.ers.usda.gov/data-products/chart-gallery/gallery/chart-detail/?chartId=94923.

Van Oost, K., Govers, G., Desmet, P., 2000. Evaluating the effects of changes in landscape structure on soil erosion by water and tillage. Landsc. Ecol. 15, 577–589. https://doi.org/10.1023/A:1008198215674.

Verdin, K.L., 2017. Hydrologic Derivatives for Modeling and Analysis—A New global High-resolution Database, Data Series. Reston, VA. 10.3133/ds1053.

Walling, D.E., 1983. The sediment delivery problem. J. Hydrol. 65, 209–237. https://doi.org/10.1016/0022-1694(83)90217-2.

Walling, D.E., 2006. Human impact on land–ocean sediment transfer by the world's rivers. Geomorphology 79, 192–216. https://doi.org/10.1016/j.geomorph.2006.06.019.

Williams, R.J., Berndt, D.H., 1977. Sediment yield prediction based on watershed hydrology. Trans. ASAE 20, 1100–1104. https://doi.org/10.13031/2013.35710.

Wu, L., Liu, X., Ma, X.-Y., 2018. Research progress on the watershed sediment delivery ratio. Int. J. Environ. Stud. 75, 565–579. https://doi.org/10.1080/00207233.2017.1392771.

Yang, D., Kanae, S., Oki, T., Koike, T., Musiake, K., 2003. Global potential soil erosion with reference to land use and climate changes. Hydrol. Process. 17, 2913–2928. https://doi.org/10.1002/hyp.1441.

Zema, D.A., Labate, A., Martino, D., Zimbone, S.M., 2017. Comparing different infiltration methods of the HEC-HMS model: the case study of the Mésima Torrent (Southern Italy). L. Degrad. Dev. 28, 294–308. https://doi.org/10.1002/ldr.2591.